

OPEN ACCESS

Wind turbine control applications of turbine-mounted LIDAR

To cite this article: E A Bossanyi *et al* 2014 *J. Phys.: Conf. Ser.* **555** 012011

View the [article online](#) for updates and enhancements.

You may also like

- [Eye-safe photon counting LIDAR for magmatic aerosol detection](#)
Vladimir A Zavozin, Mikhail Ya Grishin, Vasily N Lednev et al.
- [Recent applications of novel laser techniques for enhancing agricultural production](#)
Mohammad Nadimi, Da-Wen Sun and Jitendra Paliwal
- [A new algorithm for the extrinsic calibration of a 2D LIDAR and a camera](#)
Lipu Zhou and Zhidong Deng



PRIME
PACIFIC RIM MEETING
ON ELECTROCHEMICAL
AND SOLID STATE SCIENCE

HONOLULU, HI
Oct 6–11, 2024

Abstract submission
deadline extended:
April 19, 2024
Learn more and submit!

Joint Meeting of
The Electrochemical Society
•
The Electrochemical Society of Japan
•
Korea Electrochemical Society

The banner features a collage of three images: a woman in a black jacket speaking into a microphone, a group of people at a conference, and a woman pointing at a poster.

Wind turbine control applications of turbine-mounted LIDAR

E A Bossanyi, A Kumar and O Hugues-Salas

GL Garrad Hassan, St. Vincent's Works, Silverthorne Lane, Bristol BS2 0QD, UK

ervin.bossanyi@gl-garradhassan.com

Abstract. In recent years there has been much interest in the possible use of LIDAR systems for improving the performance of wind turbine controllers, by providing preview information about the approaching wind field. Various potential benefits have been suggested, and experimental measurements have sometimes been used to claim surprising gains in performance. This paper reports on an independent study which has used detailed analytical methods for two main purposes: firstly to try to evaluate the likely benefits of LIDAR-assisted control objectively, and secondly to provide advice to LIDAR manufacturers about the characteristics of LIDAR systems which are most likely to be of value for this application. Many different LIDAR configurations were compared: as a general conclusion, systems should be able to sample at least 10 points every second, reasonably distributed around the swept area, and allowing a look-ahead time of a few seconds. An important conclusion is that the main benefit of the LIDAR will be to enhance of collective pitch control to reduce thrust-related fatigue loads; there is some indication that extreme loads can also be reduced, but this depends on other considerations which are discussed in the paper. LIDAR-assisted individual pitch control, optimal C_p tracking and yaw control were also investigated, but the benefits over conventional methods are less clear.

1. Introduction

Recent developments in LIDAR technology have led to much interest in the possibility of improving wind turbine control by making use of a turbine-mounted LIDAR system to sense the approaching wind field before it reaches the turbine, providing preview information which might help the controller to improve turbine performance. This could significantly reduce the loads on the turbine, leading to improved cost-effectiveness, especially for large turbines.

There have also been claims of direct increases in energy capture as a result of using such preview information, but if the controller is well designed, the scope for this is rather limited. However if loads can be reduced, this could lead to an indirect increase in energy capture, for example by allowing a larger rotor swept area for the same loading. The LIDAR thus represents an innovation which allows the entire turbine design to be re-optimised, leading to an improvement in cost-effectiveness of future designs.

This paper summarises some results of a research programme aimed at clarifying the possibilities of LIDAR-assisted wind turbine control, quantifying the potential benefits, and providing insights about the particular technical features and characteristics of LIDAR systems which are likely to be of greatest benefit in this area. The research was carried out by GH in collaboration with two leading suppliers of LIDAR systems for this application. The work is based on simulation modelling, using the 5MW UPWIND reference turbine model as an example [1]. The detailed results can be found in [13].



2. Scope of the research

The research is based on simulations using the widely-used simulation code *Bladed*. This already included some capability for modelling a LIDAR sensor, implemented during the earlier UPWIND study [2]. This was extended and refined to permit all the relevant LIDAR configurations described in Section 2.2 to be modelled in detail. It was also extended with a new model to simulate the evolution of turbulence between the point of measurement and when it reaches the turbine [7], thus avoiding the need to make the traditional assumption of frozen turbulence convecting with the mean wind speed.

A *Bladed*-compatible external controller was extended to allow one or more LIDAR beams to be manipulated, enabling scanning patterns of arbitrary complexity to be simulated. The measured LIDAR signals are then processed to estimate quantities such as wind speed, direction and shear gradients, and modifications to the baseline control algorithm were implemented to make use of these quantities to improve the control action. In future, control approaches such as Model Predictive Control may be well-suited to making use of look-ahead information from a LIDAR, but require much development effort, so this study was limited to the use of very simple feed-forward additions to the baseline controller which would be easy to implement for early field tests of the principles.

The research covered the following areas:

- Development of algorithms for processing the raw LIDAR signals,
- Initial screening of many LIDAR configurations by testing their ability to estimate rotor-averaged quantities (wind speed, direction and shear gradients),
- Development of control algorithms to make use of a few selected configurations to improve the wind turbine control action,
- Evaluating the performance of the LIDAR-assisted controllers using detailed loading simulations carried out in accordance with the IEC Edition 3 standard [14].

2.1. Possible control applications of LIDAR

Many suggestions have been made for using LIDAR to improve wind turbine control, such as:

- Improved energy capture due to better yaw tracking
- Improved energy capture due to better C_p tracking
- Reduced fatigue loads due to anticipation of approaching wind field
- Reduced extreme loads due to anticipation of extreme gusts

There are already a number of published studies of some of these aspects, for example [2] - [6]. The use of LIDAR to reduce loads through improved collective pitch control appears to offer the most obvious advantages in a relatively straightforward way, so the study concentrates particularly on this aspect, especially in terms of fatigue load reduction, although the possibility of reducing extreme loads is also discussed. The possibility of further fatigue load reduction through improved individual pitch control has also been considered, as well as the possibilities of improving peak C_p tracking and yaw tracking.

2.2. LIDAR configurations studied

Both continuous-wave (CW) and pulsed LIDAR technologies were investigated. Both systems use the Doppler shift of a reflected laser beam to measure the wind component along the beam direction, averaged along a length of the beam line, the average being weighted strongly at a set focus distance and tailing off on either side. For pulsed systems the range is determined by the time taken before the reflection is received; this means that a number of different ranges can be sampled simultaneously. For CW systems the beam is focused to given range, and the weighting function has a different form which depends on the focus distance and the parameter $\alpha = \lambda/A$, where λ is the laser wavelength and A the lens area [8]. The weighting functions used are shown in Figure 1 and Figure 2, although for the CW case the width and asymmetry change as a function of range and α .

Many different LIDAR configurations were simulated for the initial screening, with the following characteristics in various combinations:

- CW LIDAR with various focal distances and α values
- Pulsed LIDAR with various numbers of simultaneous focal distances (up to 10)
- Various sampling rates
- Single staring beam
- 2, 3, 4, 6 or 8 fixed beams (pulsed only)
- Simultaneous or sequential switching of focal distances
- Single circular scanning beam with various angles between beam and centreline, and various numbers of samples per scan
- Single beam performing rosette or Lissajous scan (see Figure 3)
- Nacelle mounted, spinner or blade mounted options

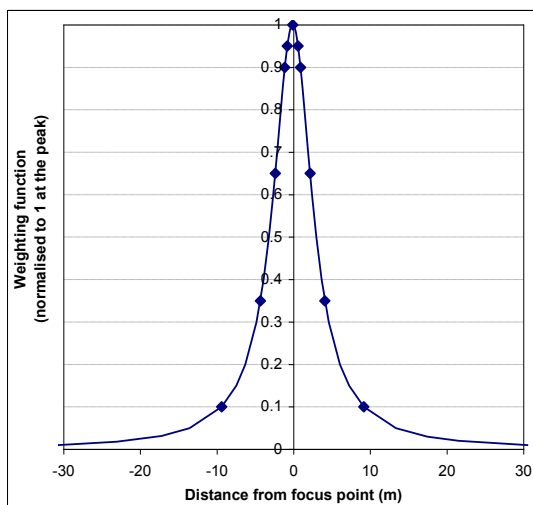


Figure 1: Example CW LIDAR weighting function

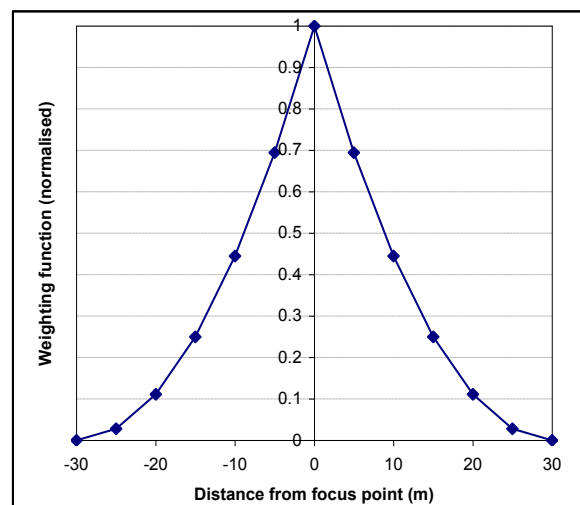


Figure 2: Example pulsed LIDAR weighting function

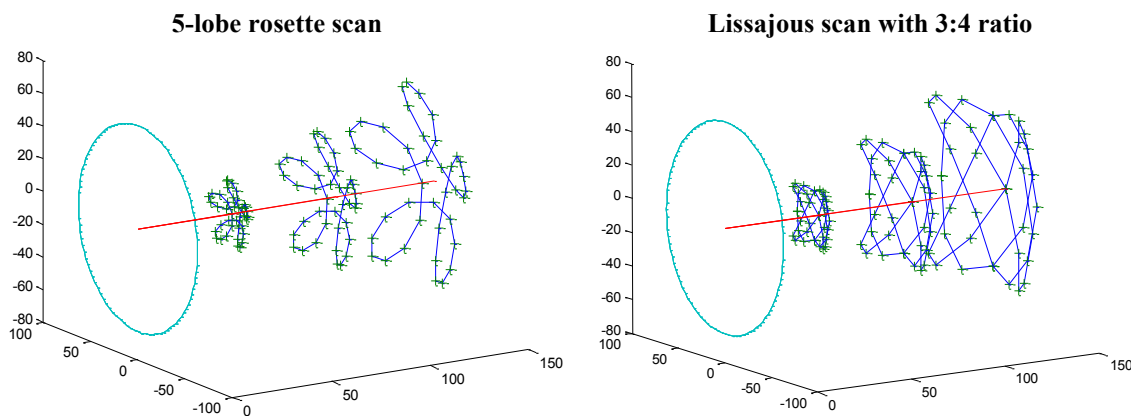


Figure 3: Scanning patterns: rosette and Lissajous

Sampling rates from 2 Hz to 50 Hz were tried for the CW system; pulsed systems tend to have lower sampling rates (between 1 Hz and 8 Hz were tried), but each sample can measure the wind speed at many points simultaneously by using multiple beams and/or multiple points per beam.

3. Estimation of rotor-averaged quantities

As the LIDAR measures only the wind speed component along the beam, assumptions have to be made about the wind field to convert a series of point measurements into wind field estimates. It is also very difficult to distinguish between wind speed gradients and flow angles. Many possible algorithms were tried, before selecting a least-squares fitting method based on assumptions about

uniform flow with linear vertical and horizontal shear gradients [13]. These gradients were separated from direction changes by assuming that significant direction changes occur at low frequency, while horizontal shear changes faster; and upflow is assumed to be known as a function of the location and the gross wind direction. This algorithm results in estimates of the longitudinal wind speed, vertical and horizontal shear gradients, and wind direction.

The configurations were compared in terms of the rms error between the LIDAR estimate and the true rotor-averaged quantity, i.e. longitudinal wind speed, vertical or horizontal shear gradient and direction. Not surprisingly, the best configuration is not the same for each of these measures. The performance of the best configuration in each case is illustrated in Figure 4 to Figure 7. This is for a 10-minute simulation with 13 m/s mean wind speed and turbulence defined according to the IEC Edition 3 standard for class 1A conditions, although to exercise the direction estimation more fully, a 10-minute $+15^\circ$ sinusoidal wind direction transient was superimposed on the flow. The black line is the true rotor-averaged quantity, with the LIDAR estimate in red.

From the large number of configurations tested, some general conclusions can be drawn out, starting with the more obvious ones:

- Good coverage of the rotor swept area is important, whether by scanning or by using multiple sample points (distances and/or separate beams), but there is inevitably a trade-off between the number of points sampled and the time taken to sample them all. The more complex scan patterns do not seem to provide any particular advantage compared to a simple circular scan. A reasonable target might be to sample the swept area once per second, using about ten well-distributed points. More samples and/or faster sampling are always beneficial, but there are diminishing returns beyond this point.
- Within the studied range of 15° - 45° , the larger the angle between the beam(s) and the centreline, the better the estimation of wind direction, and the worse the estimation of longitudinal wind speed and shear gradients.
- A sharply-focussed measurement is not always advantageous, perhaps because a more distributed sample along an angled beam is representative of more of the swept area – but of course the resolution in terms of look-ahead time will be less precise.
- A spinner-mounted LIDAR is as effective as a nacelle-mounted LIDAR, as it is easy to correct for rotor azimuth and shaft tilt in the processing (and it avoids the problem of blockage by the passing blades). A fixed blade-mounted system can also give similar results – in this case a beam emitted from a point on just one blade at 70% radius was used.
- For longitudinal wind speed, the smallest rms errors were around 0.5 m/s at 13 m/s mean wind speed. A single fixed beam typically achieved an rms error of 1.2 m/s.
- Assuming the mean upflow is known, the smallest rms errors for vertical shear gradient were around 0.013s^{-1} when the actual rms vertical shear was around 0.0375s^{-1} (consisting of a mean offset of 0.03s^{-1} due to the 0.2 wind shear exponent and a standard deviation of 0.022s^{-1}).
- For horizontal shear, the error is larger due to the difficulty of distinguishing horizontal shear from wind direction. The actual rms shear was 0.019s^{-1} (with zero mean) and the lowest rms errors obtained were around 0.02s^{-1} . The errors were lowest when the wind direction was near to zero, as might be expected, indicating that if the turbine yaw control is effective, the estimation would be better than in these simulations which did not include any yaw control.
- For wind direction, the best configurations achieved an rms error of around 4.5° compared to an actual rms direction variation of 10° (again with zero mean).
- Different configurations are best for estimating wind speed, shear gradient or direction, so the optimum choice of configuration would depend on the relative importance of different control objectives in any particular wind turbine design.

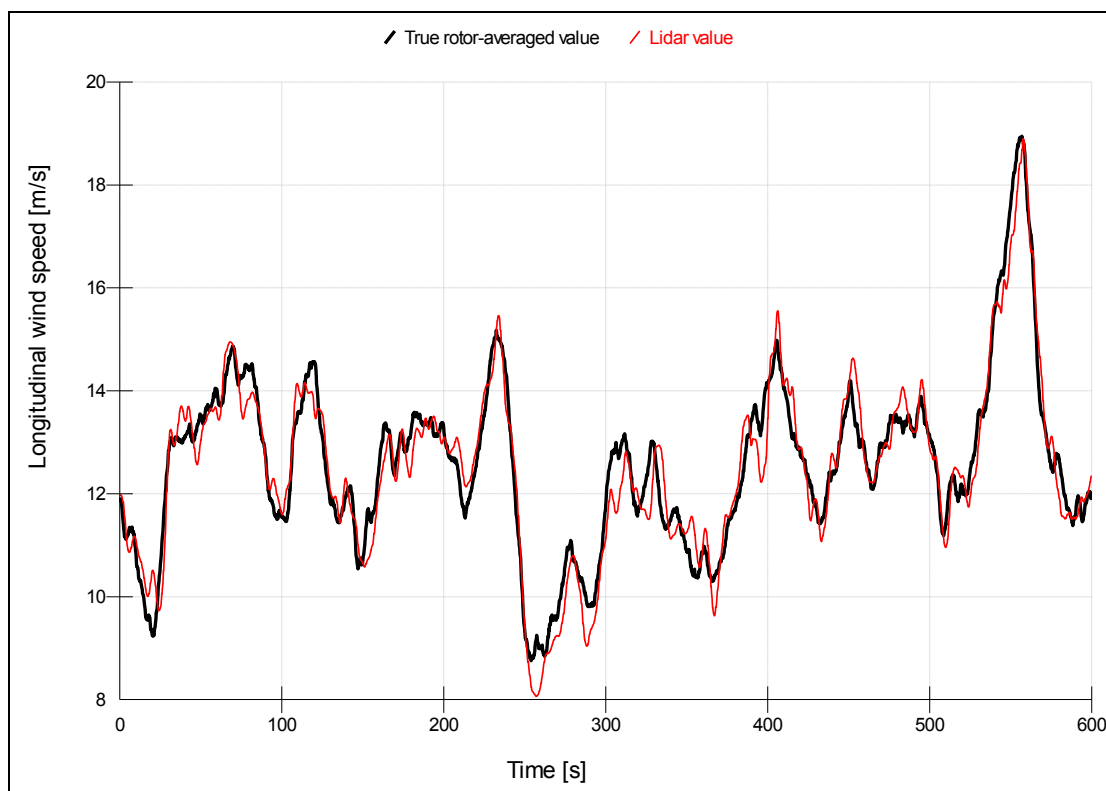


Figure 4: LIDAR prediction of longitudinal wind speed

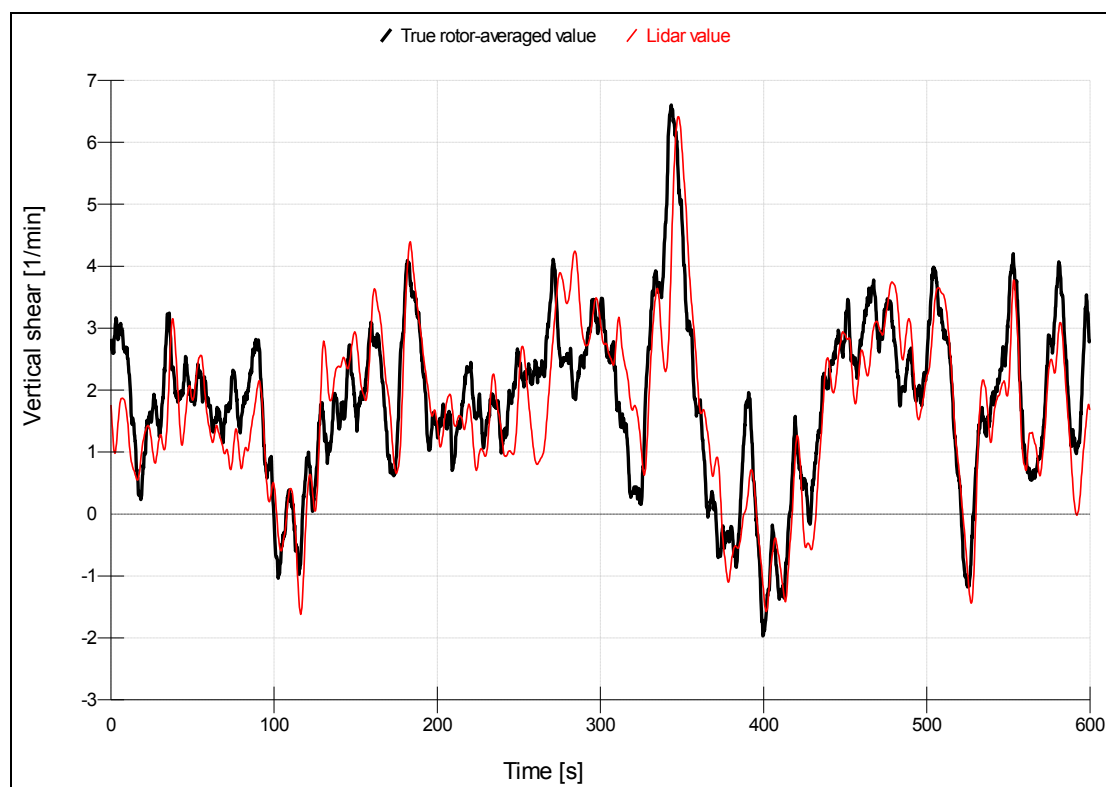


Figure 5: LIDAR prediction of vertical shear gradient

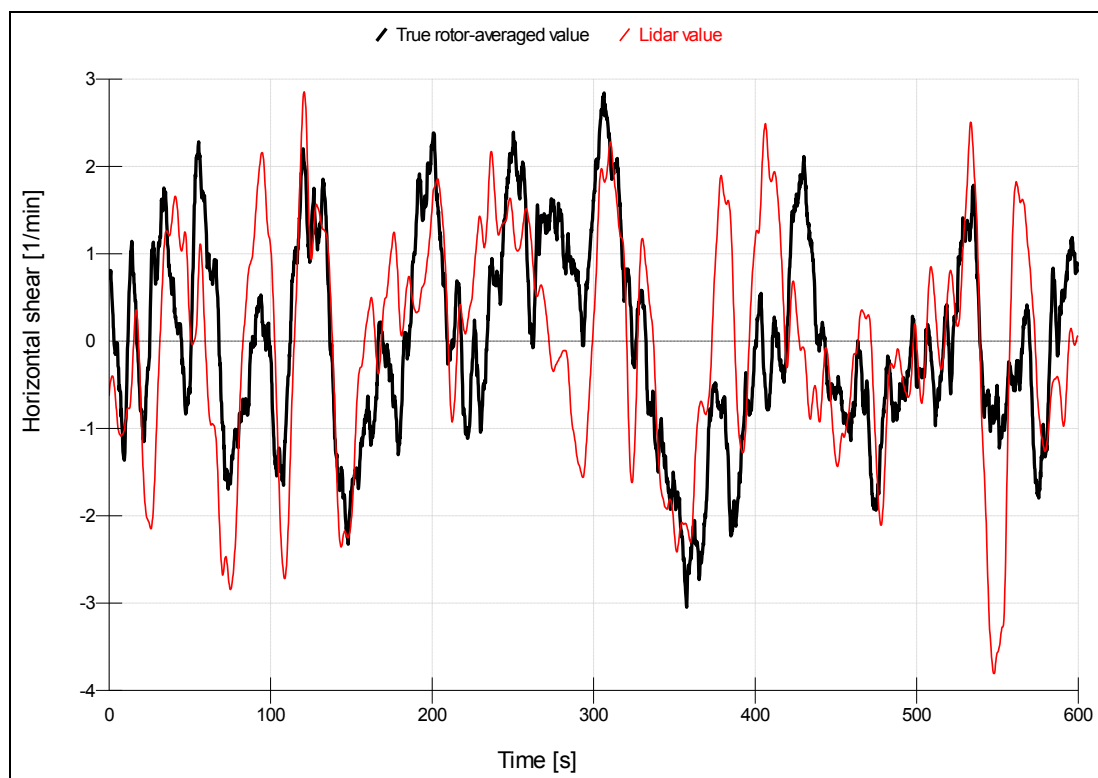


Figure 6: LIDAR prediction of horizontal shear gradient

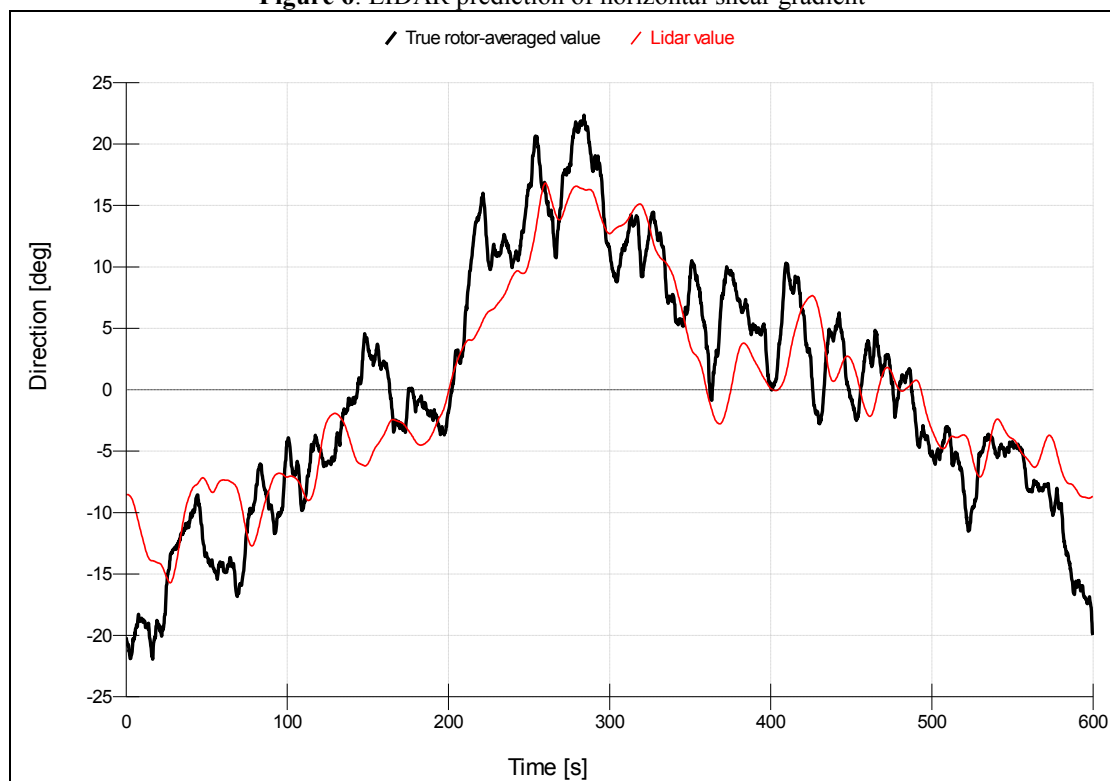


Figure 7: LIDAR prediction of wind direction

Since these results are all for one particular 10-minute turbulence history, a few runs were repeated with a different random number seed (giving a different realisation of turbulence with the same spectral properties), and also with different mean wind speeds (9 m/s and 21 m/s), and with more typically offshore wind conditions (half the turbulence intensity and half the wind shear). Clearly the actual rms deviations scaled with the wind speed, turbulence intensity and shear as expected, but the rms errors in LIDAR predictions scaled in a very similar way, so the above conclusions are not affected.

4. Collective pitch control enhancement

Previous studies, for example [2] - [6], have already shown that LIDAR preview measurement of longitudinal wind speed may help improve collective pitch control action – this is used principally to regulate the rotor speed to the rated value when operating above rated wind speed, i.e. once rated power has been reached. However, any change to the pitch angle also has a major effect on rotor thrust, and hence on out of plane blade loads, tower vibration, tower bending moments, etc. The collective pitch controller design involves a compromise between tight speed regulation and turbine loads, especially tower moments. Relatively high-frequency pitch action is needed to minimise loads, while speed regulation can be achieved with lower bandwidth because of the large rotor inertia. The LIDAR preview information is well-suited to driving this low-frequency action, effectively freeing up the higher-frequency action to concentrate on load alleviation.

A simple feed-forward scheme fairly similar to that in [2] was used, in which an additional collective pitch rate is calculated as $(\theta_T - \theta)/T$ where θ_T is the steady-state pitch angle corresponding to the LIDAR-measured wind speed at look-ahead time T and θ is the current pitch angle. More sophisticated approaches e.g. using model-inverse approaches [5] were not considered. The LIDAR feed-forward is combined with the conventional PI-based speed regulation feedback controller; it takes over some of the low-frequency speed regulation duty, so the PI controller can be reoptimised by reducing the gains, such that the speed control is still as good but a reduction in pitch activity and thrust-related loads is achieved. The effects of look-ahead time and low-pass filtering of the LIDAR signal were also investigated. As indicated in [7], severe filtering is not needed as long as the effects of decorrelation of the wind field between the measurement point and the turbine are properly accounted for.

4.1. Illustration of the LIDAR feed-forward scheme

To illustrate the above principles, simulations have been carried out using IEC turbulent wind conditions as before, with a mean wind speed of 13 m/s. Zero mean yaw misalignment was used (and no sinusoidal direction transient), as the effectiveness of the LIDAR in estimating the longitudinal wind speed is not much affected by wind direction. LIDAR configurations, both pulsed and continuous-wave, were selected for good longitudinal wind speed estimates, and used with appropriate look-ahead times which are mostly around 5 seconds (although this was not systematically optimised).

Four cases are shown for illustration, as listed in Table 1. This also shows the rotor speed statistics obtained using one particular LIDAR configuration (30° circular scan at 75m range). This shows that the addition of LIDAR in case (b) tightens the speed control, but if the PI gains are reoptimised as in case (c) the original quality of speed control is approximately restored. Without the LIDAR, the reoptimised gains are not acceptable as the speed control is now too slack – case (d). Figure 8 shows the rotor speed time histories.

		Max RPM	RPM Std.Dev.
(a) Base PI	Base case with no LIDAR	12.71	0.40
(b) Base PI + Lidar	LIDAR feed-forward added	12.35	0.35
(c) Reopt + Lidar	As (b) but with reduced PI feedback gains	12.52	0.39
(d) Reopt, no Lidar	Reduced PI gains as in (c) but no LIDAR	13.52	0.64

Table 1: Four test cases, and sample rotor speed statistics for one configuration (13 m/s simulation)

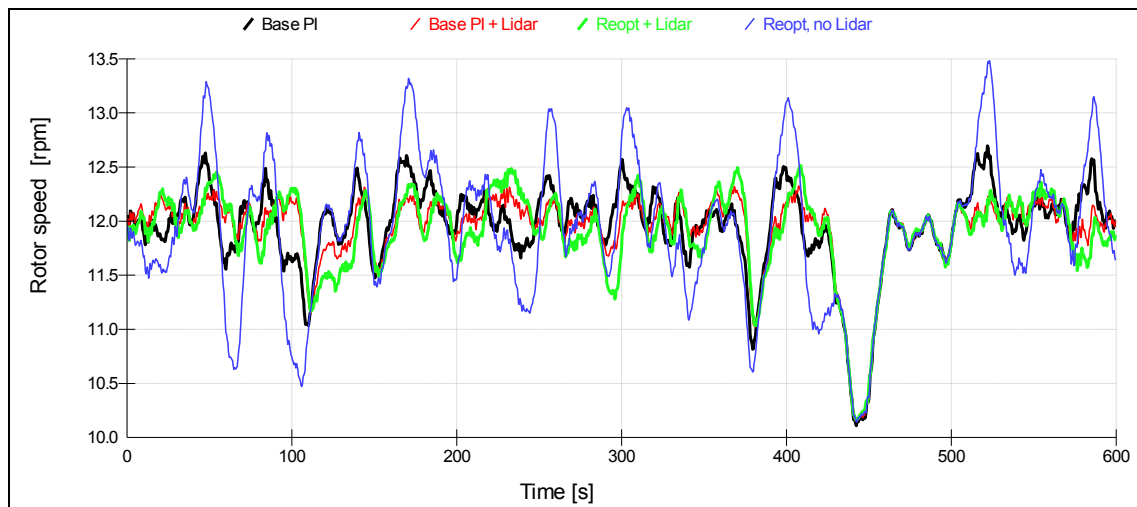


Figure 8: Rotor speed time histories (13 m/s simulation)

Figure 9 compares the collective pitch angle (mean of the three blades) for case (c) against the base case. In the LIDAR case the pitch control is significantly calmer, and appears to ride through wind disturbances in the way we might expect given the advance information which is available. The effect of the reduced pitch activity is to reduce vibrations and loads elsewhere in the turbine. In particular, fore-aft tower vibration is much reduced as shown by the tower base bending moment in Figure 10.

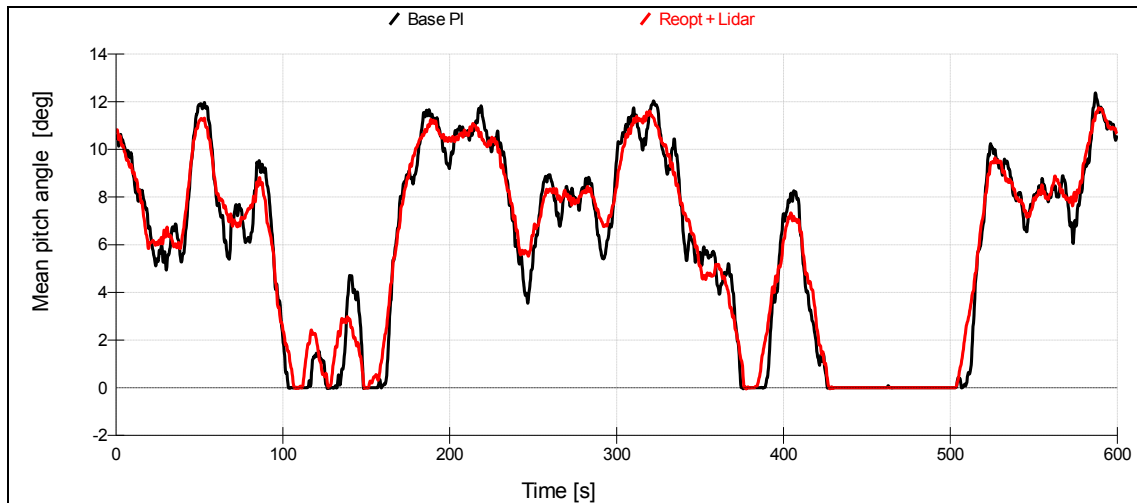


Figure 9: Collective pitch angle (13 m/s simulation)

4.2. Fatigue loads

To evaluate the overall effect of the LIDAR in terms of fatigue load reduction, a complete set of fatigue loads defined according to the IEC Edition 3 for class 1A wind conditions (10 m/s annual mean wind speed) was run with and without the LIDAR (cases (a) and (c) above). This included both operational and non-operational load cases. The total lifetime damage equivalent loads (DELs) for key components were calculated – this is a useful comparative measure of fatigue, being the amplitude of a sinusoidal variation which would cause the same amount of fatigue damage, given the properties of the material defined in terms of the Wöhler exponent or ‘inverse S-N slope’, for which values of 4 and

10 have been used to represent steel and glass-reinforced plastic (GRP) components respectively. All loads are defined with respect to the GL co-ordinate system as described for example in [15].

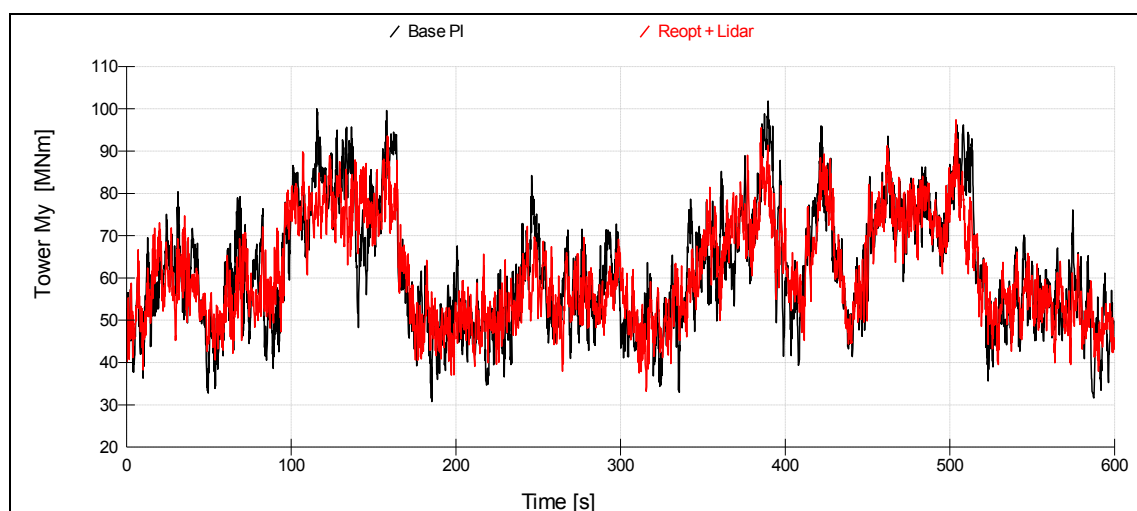


Figure 10: Tower base moment (13 m/s simulation)

Lifetime DEL results are shown in Figure 11, where the hatching indicates the range of values obtained with different LIDAR configurations. The most important results for the turbine design are the reduction in thrust (Fx) and hence in tower base My (fore-aft bending moment), also blade root My (out of plane bending moment) and Mz (pitching moment, reflecting lower pitch activity). Other loads are unchanged or slightly reduced, with only one very slight increase, in tower side-side force in some cases. Note that only the operational cases around and above rated wind speed are affected by the LIDAR, so the beneficial effect is inevitably diluted by the contribution from below-rated wind speeds and other load cases unaffected by the LIDAR, such as non-operational cases. In high wind operation, blade root My was typically reduced by 6 – 12 % and tower base My by 16 – 20%.

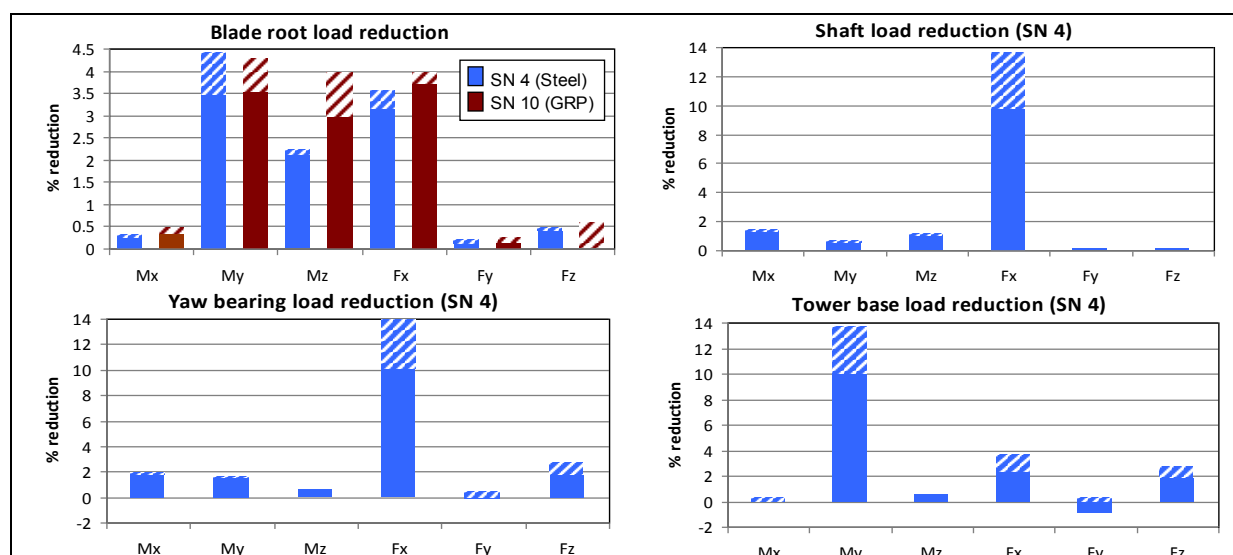


Figure 11: Lifetime fatigue load reductions

4.3. *Extreme loads*

This LIDAR action reduces fatigue loads, so it is reasonable to ask whether it could also reduce extreme loads. A number of studies (for example [2]) have already demonstrated massively improved response to the ‘Mexican hat’ extreme coherent gust used in some standard extreme load cases. However this does not necessarily mean that the LIDAR allows the turbine to be designed to a reduced extreme load envelope, for a number of reasons:

- Such gusts are physically unrealistic, but are included in the standards as a simple way of generating abnormal load levels which the turbine should be designed to withstand. If prior knowledge of the gust is used to mitigate these loads, it could be argued that more efforts should be made to identify other possible sources of such abnormal loads. Existing standards did not anticipate the use of LIDARs for control, and they should not be used blindly.
- One has to assume that the extreme gust convects unchanged towards the turbine at a known velocity, but this is undefined, especially for a gust which does not return to the starting wind speed. Some of the most severe standard gusts also involve a large direction change, so the gust’s direction of movement is also undefined – it might move sideways and miss the turbine, or a gust might approach the turbine from the side, undetected by a forward-facing LIDAR. Such events are quite possible, e.g. in thunderstorm fronts, large topographical-scale eddies or low-level jets. A large horizontal eddy contains all possible directions, and its direction of movement cannot be ascertained by measuring the wind direction in that part of the eddy which happens to be in front of the turbine.
- Even if the LIDAR can reduce the loading during an extreme gust, the design can only take advantage of this if the LIDAR is guaranteed to be working when the extreme gust occurs. LIDAR faults would only have to be considered together with a one-year gust; but the LIDAR signal could also be affected by fog, precipitation or a lack of aerosol particles, in which case the probability of this coinciding with a 50-year gust would have to be considered.
- Although extreme gusts can generate large loads, they are not necessarily design-driving loads if larger loads are generated as a result of fault cases for example.

In any case, later standards make less use of extreme coherent gusts in determining extreme loads. In Edition 3 of the IEC standard, they are now only used in combination with events such as faults and grid loss, and operational extreme loads are determined by statistical extrapolation from a normal operational design load case (DLC 1.1). The highest extremes are found, and the probability of occurrence in a 10-minute dataset is calculated from the distribution of extremes in each wind speed bin, and weighted by the probability of occurrence of the bin according to the annual wind speed distribution. DLC 1.1 was run for the base case and two different LIDAR configurations, and the results are shown in Figure 12 for blade root M_y and Figure 13 for tower base M_y . An extreme probability distribution curve (not shown) would be fitted to this data and extrapolated to give a ‘once in 50 years’ extreme load, which corresponds to a probability level of 3.8×10^{-7} . This would certainly result in a lower extreme tower base moment in the LIDAR cases. There may be a smaller reduction for the blade root load.

This analysis did not reveal any systematic change in other extreme loads. However it did reveal the need for yet more care in the analysis to avoid misleading pitfalls, especially those resulting from supervisory control. For example, there were some increased extreme loads due to avoidable shut-downs caused by supervisory control trips which had not been re-tuned to account for the LIDAR. This is typical of the sort of issues which arise during extreme loads analysis, and demonstrates that it only really makes sense to examine the extreme loads as part of a complete design exercise.

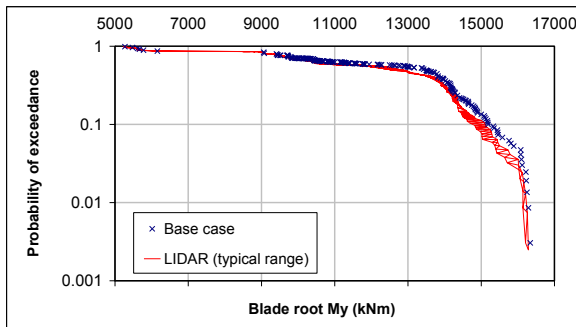


Figure 12: Extreme load reductions: Blade root My

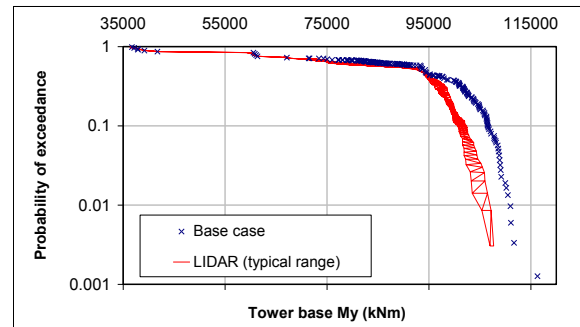


Figure 13: Extreme load reductions: Tower base My

5. Individual pitch control enhancement

The use of turbine-mounted LIDAR has also been suggested for improving individual pitch control (IPC), e.g. [9], [10]. Standard 1P-IPC as in [1] generates once-per-revolution individual pitch demand increments at each blade to offset the effect of a linear wind speed gradient across the rotor, which can be represented by lateral and vertical wind shear gradients; so if these gradients can be measured by the LIDAR, they may help to improve the IPC action. The standard IPC action uses PI controllers for the horizontal and vertical shear compensation, so a LIDAR feed-forward technique can be used in a very similar way to the collective pitch case. In this case there is no need to reoptimise the PI gains, since both feed-forward and feedback controllers control the relatively slowly-varying asymmetric loads without the side-effects of tower excitation. Setting zero gain gives LIDAR-only IPC action.

Two LIDAR configurations (CW and pulsed), selected for good performance in estimating shear gradients, were tested with the same 13 m/s wind conditions. Four cases were run: No IPC, LIDAR IPC, conventional IPC, and LIDAR-assisted conventional IPC. Table 2 shows that the LIDAR IPC reduces loads: less than conventional IPC, with a correspondingly smaller amount of additional pitch activity. LIDAR-assisted conventional IPC gives a very small improvement compared to conventional IPC only. The ranges indicate the spread of values obtained with different LIDAR configurations. Note that the conventional IPC includes both 1P and 2P IPC. 1P IPC causes most of the rotating (blade and shaft) load reduction, while 2P IPC causes most reduction at the tower top. The LIDAR IPC did not include any 2P action, although in principle this should be possible.

Another advantage of the conventional feedback approach for this application is that it directly measures the loads which it is trying to reduce, compared to the LIDAR feed-forward method which uses a measure of the wind gradients which is both indirect and imperfect.

	Conventional IPC	LIDAR IPC	LIDAR-assisted conventional IPC
Blade root out-of-plane moment (steel)	30.4%	11 – 15%	30.6 – 30.8%
Blade root out-of-plane moment (GRP)	31.3%	16 – 19%	32.2 – 32.3%
Shaft My bending moment (steel)	41.4%	12 – 18%	41.3 – 41.4%
Shaft Mz bending moment (steel)	40.5%	12 – 18%	40.6 – 40.8%
Tower top nod moment (steel)	19.9%	4 – 7%	20.6 – 20.8%
Tower top yaw moment (steel)	14.1%	3 – 8%	13.8 – 14.1%
Increase in pitch travel	127%	62-65%	123%

Table 2: Fatigue load reductions and increase in pitch action due to IPC at 13 m/s

6. C_p tracking enhancement

Another way in which LIDAR wind preview information could conceivably improve turbine performance is by helping to maximise energy capture in below-rated winds by maintaining optimum tip speed ratio to maximise aerodynamic efficiency of the rotor (C_p). This is normally done very simply by demanding a generator torque proportional to the rotor speed squared so that the rotor speed

varies in proportion to the wind speed, but the large rotor inertia will result in a following error. A few seconds' LIDAR preview information should allow trajectory planning to minimise this error, as suggested for example in [11]. Figure 14 shows that the rotor speed can indeed be made to track the rotor-averaged wind speed better, but at the expense of unacceptable power and torque variations needed to achieve the high accelerations (Figure 15). In this simulation the mean power increased by only 0.2%, and this is only available in wind speeds between about 6 and 10 m/s; the annual energy capture increase would be much smaller.

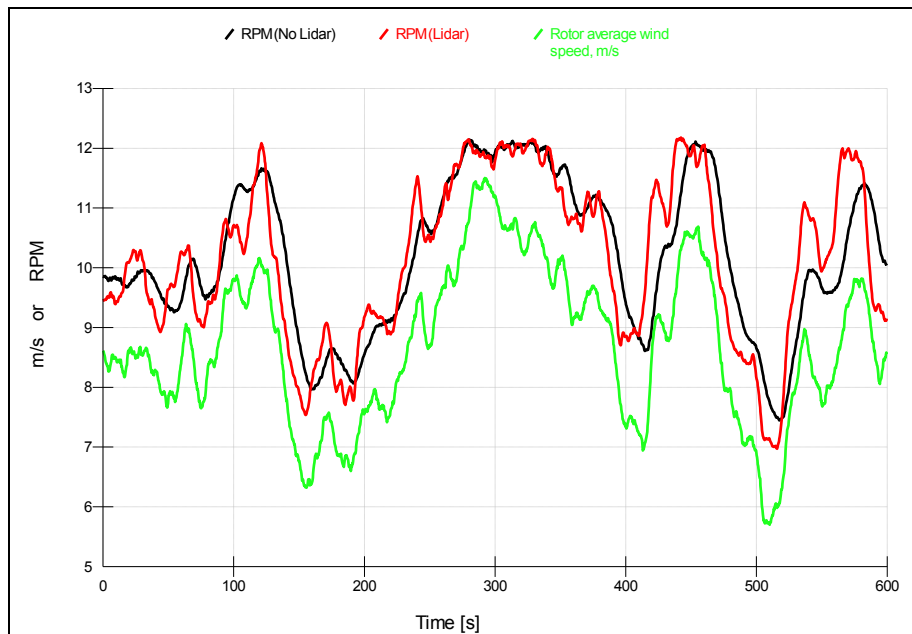


Figure 14: Rotor speed from 9 m/s simulation, with rotor-average wind speed for comparison (green)

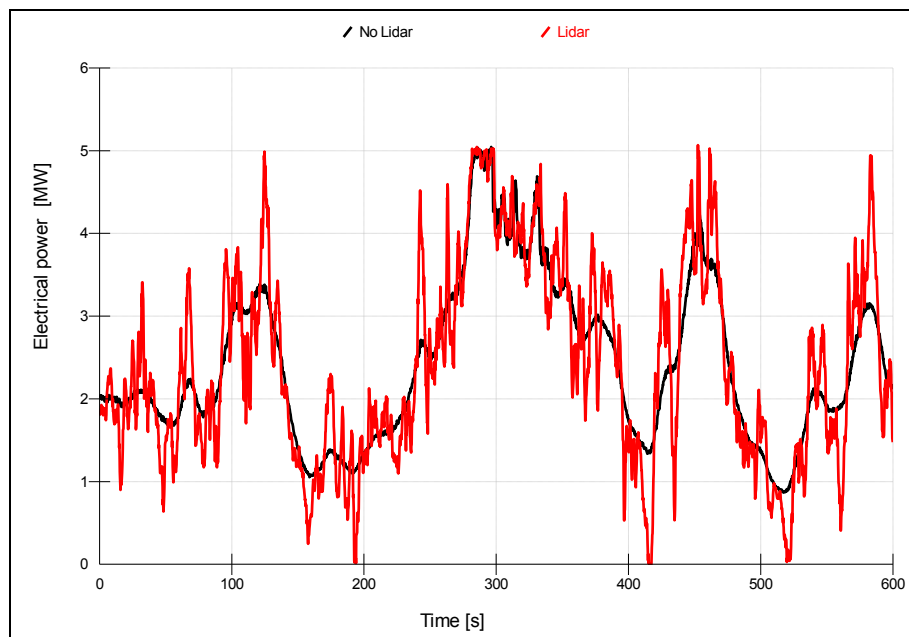


Figure 15: Power output from 9 m/s simulation

7. Yaw control enhancement

Conventional yaw control uses a nacelle-mounted wind vane to measure yaw misalignment. Heavy filtering is needed to average out local fluctuations; but yaw control has to be slow anyway to avoid high yaw actuator and gyroscopic rotor loads. Local flow patterns may lead to bias errors, but in principle these can be corrected by careful calibration as a function of operating point [12]. A LIDAR can be an effective instrument for measuring yaw misalignment, and could therefore be a valuable tool for performing this calibration, for example during commissioning, but it is not clear that a permanent turbine-mounted LIDAR would necessarily maintain better yaw control thereafter. Standard 10-minute simulations are inadequate for investigating this in detail, as yaw control time constants are too long, and are exercised by lower-frequency direction variations than the turbulence spectra describe – they may even be quite site-dependent. Some simulations were carried out just to illustrate the nature of the trade-offs (Figure 16). The LIDAR showed no obvious advantage, but this result is far from definitive.

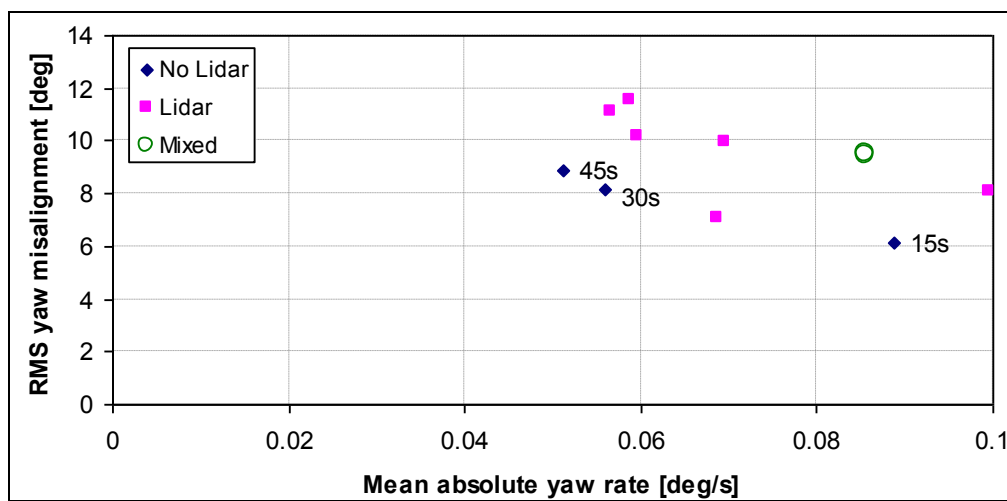


Figure 16: Yaw tracking: trade-off between tightness of yaw tracking and yaw actuator duty as a function of different yaw error filtering strategies with 10° yaw error deadband. No Lidar: yaw error averaging time is given. Lidar: various different yaw error filters. Mixed: mean of 15s averaged wind vane signal and 0.05 rad/s second-order filtered Lidar signal

8. Conclusions

A detailed analytical study has shown that fatigue and probably some extreme loads can be reduced significantly, even using very simple control strategies, by enhancing collective pitch control using a turbine-mounted LIDAR providing a few seconds' look-ahead time. The same LIDAR could also provide a small amount of load reduction through individual pitch control without the additional load sensors, although a somewhat more sophisticated approach may be worth pursuing here to improve the effectiveness. The prospects for LIDAR-enhanced C_p tracking and yaw control are much less clear.

Both pulsed and continuous-wave LIDAR types are suitable, as long as they can sample something like 10 points distributed around the swept area every second or so and provide a few seconds of look-ahead time.

9. Acknowledgements

This study was partly funded by contributions from LIDAR suppliers Natural Power and Avent Lidar Technology, which are gratefully acknowledged. Detailed and open discussions with Mike Harris, Chris Slinger, Samuel Davoust and Thomas Velociter were invaluable for this work.

References

- [1] E A Bossanyi and D V Witcher, Controller for 5MW reference turbine, 10th July 2009, www.upwind.eu/pdf/D%205.1.1.%20Controller%20for%205MW%20reference%20turbine.pdf.
- [2] D Schlipf *et al*, LIDAR assisted collective pitch control, UPWIND deliverable 5.2, www.upwind.eu/pdf/D.5.1.3.%20LIDAR%20assisted%20collective%20pitch%20control.pdf.
- [3] D Schlipf, T Fischer, C E Carcangiu, M Rossetti, and E Bossanyi, Load Analysis of Look-Ahead Collective Pitch Control Using LIDAR, 2010, *Proc. DEWEK, Bremen, Germany*,
- [4] J Laks *et al*, Blade Pitch Control with Preview Wind Measurements, 2010, *Proc. 48th AIAA Aerospace Sciences Meeting, Orlando, Florida*.
- [5] N Wang *et al*, FX-RLS-Based Feedforward Control for LIDAR-Enabled Wind Turbine Load Mitigation, *IEEE Transactions On Control Systems Technology*.
- [6] F Dunne *et al*, Adding Feedforward Blade Pitch Control for Load Mitigation in Wind Turbines: Non-Causal Series Expansion, Preview Control, and Optimized FIR Filter Methods, 2011, *Proc. 49th AIAA Aerospace Sciences Meeting, Orlando, Florida*.
- [7] E A Bossanyi, Un-freezing the turbulence: improved wind field modelling for investigating Lidar-assisted wind turbine control, 2012, *Proc EWEA Annual conference, Copenhagen, Denmark..*
- [8] E Simley *et al*, Analysis of Wind Speed Measurements using Continuous Wave LIDAR for Wind Turbine Control, 2011, *Proc. 49th AIAA Aerospace Sciences Meeting, Orlando, Florida*.
- [9] D Schlipf, *et al*, Look-ahead cyclic pitch control using lidar, Torque from Wind Third Conference, Greece, 28–30 June 2010; 1–7.
- [10] K A Knud and M H Hansen, Individual Pitch Control Based on Local and Upstream Inflow Measurements, 2012 *Proc. 50th AIAA Aerospace Sciences Meeting, Nashville, Tennessee*.
- [11] D Schlipf *et al.*, Prospects of optimization of energy production by LiDAR assisted control of wind turbines. Presentation at EWEA, 2011.
- [12] K A Kragh and P A Fleming, Rotor Speed Dependent Yaw Control of Wind Turbines Based on Empirical Data, 2012, *Proc. 50th AIAA Aerospace Sciences Meeting, Nashville, Tennessee*.
- [13] E A Bossanyi, Assessment of turbine-mounted lidar for control applications, 2012, *GL Garrad Hassan report 110062/Lidar/BR/01 (available from the author)*.
- [14] IEC, Wind turbines – Part 1: Safety requirements, international standard 61400-1 (3rd edition), *International Electrotechnical Commission, 2005*.
- [15] T Burton *et al.*, Wind Energy Handbook, *John Wiley & Sons Ltd., Second edition 2011*.